Supporting Information for Manuscript B516757D

1. UV-Vis absorption spectra

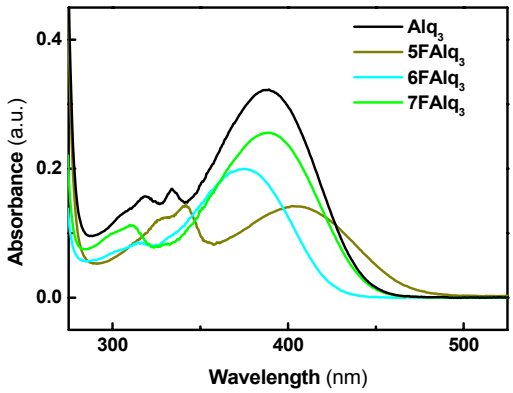

Figure S1 UV-Vis spectra of Alq_3, $5FAlq_3$, $6FAlq_3$ and $7FAlq_3$ in $CHCl_3$ solutions (~1×10^{-5} M).

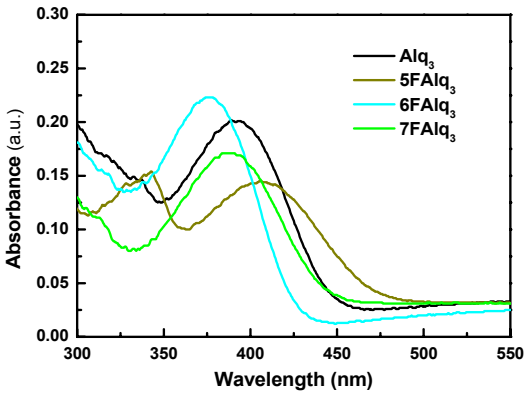

Figure S2 UV-Vis spectra of Alq_3, $5FAlq_3$, $6FAlq_3$ and $7FAlq_3$ thin films vacuum-deposited on the quartz substrates (~50 nm thick).

2. Geometric isomers

^{1}H NMR spectra of Alq_3 and its fluorinated derivatives solutions in $CDCl_3$ were obtained on a Bruker AVANCE DMX500 nuclear resonance spectroscope (500 MHz) under ambient conditions. From these spectra (Figures S4-S7), it is concluded that Alq_3 and its fluorinated derivatives obtained in this work (purified twice by temperature gradient sublimation) are all meridianal isomers, in which three hydroquinoline ligands are inequivalent by geometric symmetry, i.e. each ligand is distinguishable, leading to the splitting of the NMR peak of each hydrogen atom, especially those H atoms located on the pyridyl ring (H2, H3 and H4, see Figure S3).

Detailed assignments of NMR peaks of *mer*-Alq_3 can be found in the work reported by M. Utz et al. (*J. Am. Chem. Soc.*, 2003, V125, p1371). Our results are in perfect consistence with theirs.

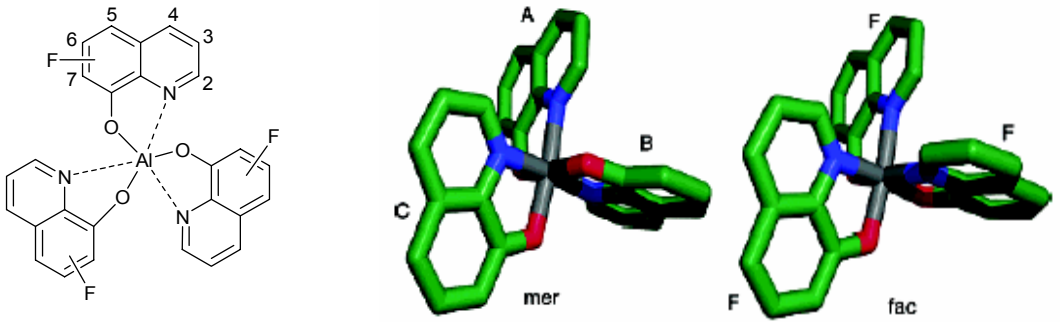

Figure S3 Molecular structures of Alq_3 and its fluorinated derivatives (left), and 3D schematics of the meridianal and facial isomers (right).

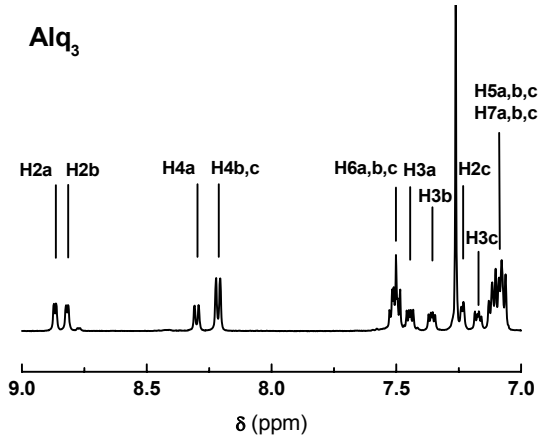

Figure S4 ^{1}H NMR spectrum of Alq_3 solution in $CDCl_3$.

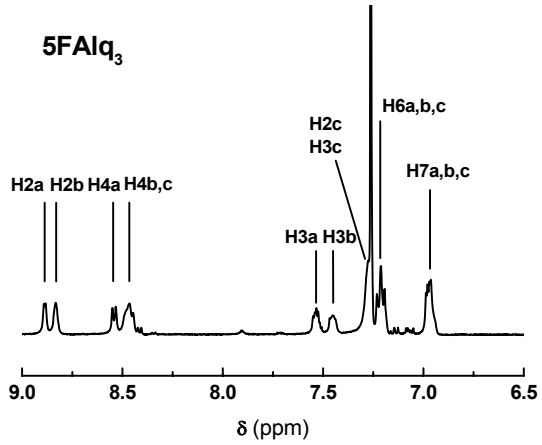

Figure S5 ^{1}H NMR spectrum of $5FAlq_3$ solution in $CDCl_3$.

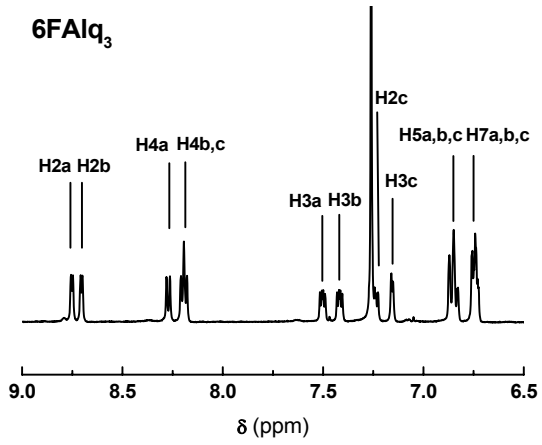

Figure S6 ^{1}H NMR spectrum of $6FAlq_3$ solution in $CDCl_3$.

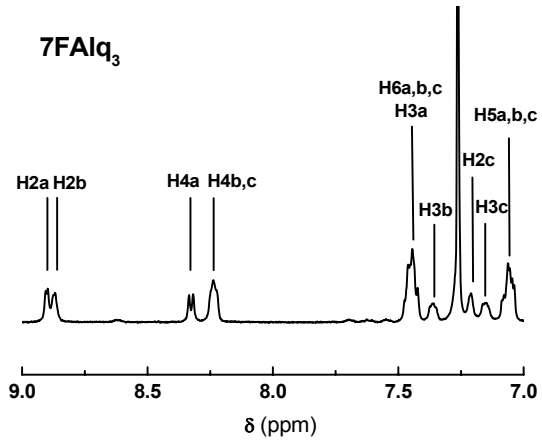

Figure S7 ^{1}H NMR spectrum of $7FAlq_3$ solution in $CDCl_3$.

It had been demonstrated that *mer*-Alq_3 can be transformed to *fac*-Alq_3 by annealing, resulting in an exothermic phase transition at ~ 380 ^{o}C in the DSC curve (*Adv. Funct. Mater.*, 2003, V13, p108). In our experiments, we also observed this phenomenon. However, the phase transition peaks of fluorinated Alq_3 derivatives could not be found. Furthermore, the vacuum-deposited films of Alq_3 and its fluorinated derivatives are all amorphous (because there are no diffraction peaks in XRD patterns). Therefore, in our case, the effect of fluorination position on the optical properties of Alq_3 originates from different molecular electronic structures instead of stereo isomerization or crystal polymorphs.

3. Fluorescence efficiencies in thin films

Alq_3 and its fluorinated derivatives were vacuum evaporated at a pressure below 1×10^{-5} Torr onto glass substrates (30 mm × 30 mm), and the deposition rate was 1-2 Å/s. All obtained thin films were 50 nm thick, monitored with a quartz crystal oscillator. Their fluorescence spectra were recorded at an excitation wavelength of 370 nm on a Hitachi 4500 fluorescence spectrophotometer. With Alq_3 as a reference, the fluorescence efficiencies of fluorinated Alq_3 derivatives in the solid state were roughly estimated by comparing their fluorescence intensity after the calibration of their absorbances at 370 nm.

4. HOMO-LUMO levels

Cyclic voltammetry (CV) measurements were carried out on a CHI600A electrochemical workstation, using millimolar solutions in CH_2Cl_2 containing 0.1M supporting electrolyte of tetrabutylammonium perchlorate in a three-electrode-cell, where Pt plate served as the working electrode, Pt wire as the counter electrode, and saturated calomel electrode (SCE) was used as the reference electrode. The scanning rate was 50 mV/s. From one-electron quasi-reversible reduction and oxidation peaks in CV curves (Figures S8-S12), the LUMO energy levels of Alq_3, $5FAlq_3$, $6FAlq_3$, and $7FAlq_3$ were calculated as -2.82, -3.06, -3.25, and -3.00 eV, respectively. It was worthy noting that the reduction and oxidation peaks of Alq_3 were not well resolved under normal scanning rate (*J. Am. Chem. Soc.*, 1998, V120, p9646), however, they became obvious in the 1st derivative of the CV curve (*Chem. J. Chinese Universities*, 2000, V21, p1422). From their absorption onsets in solutions (Figure S1), the LUMO-HOMO band gaps of Alq_3, $5FAlq_3$, $6FAlq_3$ and $7FAlq_3$ were estimated as 2.81, 2.66, 2.93 and 2.81 eV, respectively. Thus the HOMO energy levels of Alq_3, $5FAlq_3$, $6FAlq_3$, and $7FAlq_3$ were calculated to be -5.63, -5.72, -6.18, and -5.81 eV, respectively.

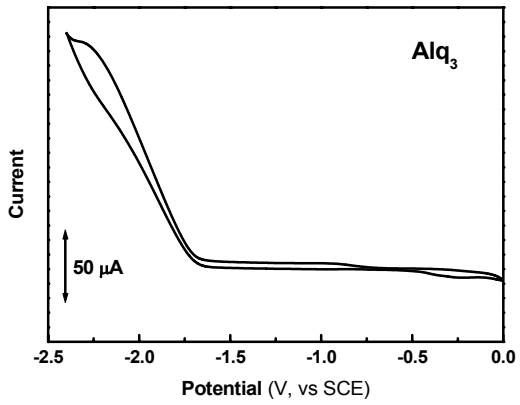

Figure S8 Cyclic voltammogram of Alq_3 solution in CH_2Cl_2.

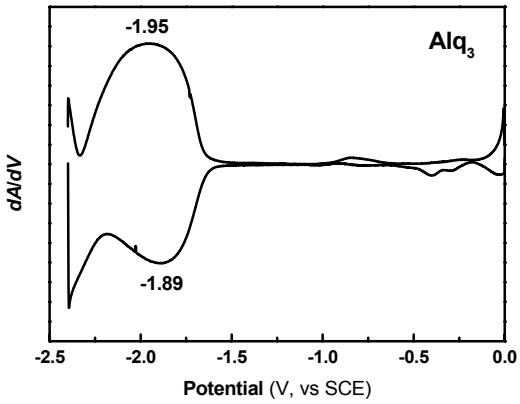

Figure S9 The 1st differential curve of cyclic voltammogram of Alq_3 solution in CH_2Cl_2.

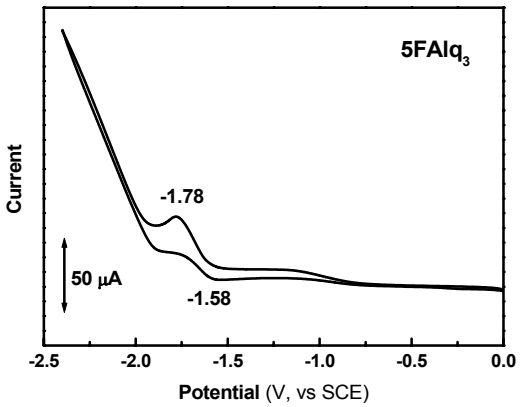

Figure S10 Cyclic voltammogram of $5FAlq_3$ solution in CH_2Cl_2.

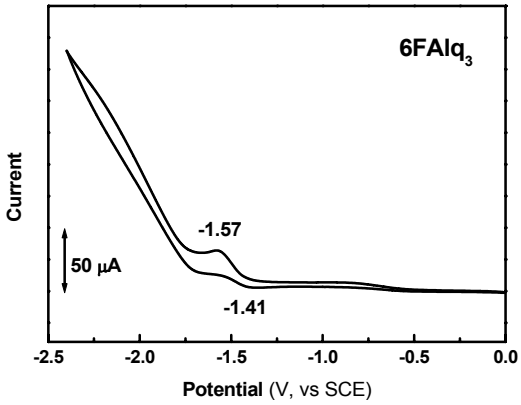

Figure S11 Cyclic voltammogram of $6FAlq_3$ solution in CH_2Cl_2.

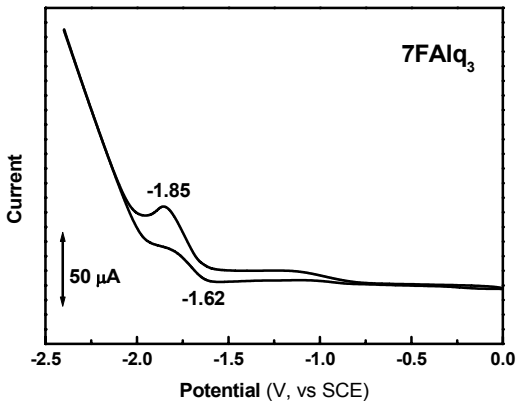

Figure S12 Cyclic voltammogram of $7FAlq_3$ solution in CH_2Cl_2.